Polarization insensitive wavelength conversion in a dispersion-engineered silicon waveguide

Pu, Minhao; Hu, Hao; Peucheret, Christophe; Ji, Hua; Galili, Michael; Oxenløwe, Leif Katsuo; Jeppesen, Palle; Hvam, Jørn Märcher; Yvind, Kresten

Published in:
Optics Express

Link to article, DOI:
10.1364/OE.20.016374

Publication date:
2012

Document Version
Publisher's PDF, also known as Version of record

Polarization insensitive wavelength conversion in a dispersion-engineered silicon waveguide

Minhao Pu,* Hao Hu, Christophe Peucheret, Hua Ji, Michael Galili, Leif K. Oxenløwe, Palle Jeppesen, Jørn M. Hvam, and Kresten Yvind

DTU Fotonik, Department of Photonics Engineering, Technical University of Denmark, Build. 343, DK-2800 Kongens Lyngby, Denmark

mipu@fotonik.dtu.dk

Abstract: We experimentally demonstrate polarization-insensitive all optical wavelength conversion of a 10-Gb/s DPSK data signal based on four-wave mixing in a silicon waveguide with an angled-pump scheme. Dispersion engineering is applied to the silicon waveguide to obtain similar four-wave mixing conversion performances for both the TE and TM modes. Bit-error rate measurements are performed and error-free operation is achieved. We also demonstrate polarization-insensitive wavelength conversion with a large separation between the idler and signal using a dual-pump configuration.

OCIS codes: (060.1155) All-optical networks; (190.4380) Nonlinear optics, four-wave mixing; (190.4390) Nonlinear optics, integrated optics; (130.7405) Wavelength conversion devices.

References and links

1. C. M. Gallep, O. Raz, and H. J. S. Dorren, "Polarization independent dual wavelength converter based on FWM in a single semiconductor optical amplifier," in *Optical Fiber Communication Conference*, OSA Technical Disgest (CD) (Optical Society of America, 2010), paper OWP2.
2. H. Hu, R. Nouroozi, R. Ludwig, B. Huettl, C. Schmidt-Langhorst, H. Suche, W. Sohler, and C. Schubert, "Polarization-insensitive all-optical wavelength conversion of 320 Gb/s RZ-DQPSK signals using a Ti:PPLN waveguide," Appl. Phys. B **101**(4), 875–882 (2010).
3. H. Hu, E. Palushani, M. Galili, H. C. H. Mulvad, A. Clausen, L. K. Oxenløwe, and P. Jeppesen, "640 Gbit/s and 1.28 Tbit/s polarisation insensitive all optical wavelength conversion," Opt. Express **18**(10), 9961–9966 (2010).
4. J. Ma, J. Yu, C. Yu, Z. Jia, X. Sang, Z. Zhou, T. Wang, and G. K. Chang, "Wavelength conversion based on four-wave mixing in high-nonlinear dispersion shifted fiber using a dual-pump configuration," J. Lightwave Technol. **24**(7), 2851–2858 (2006).
5. K. Inoue, "Polarization independent wavelength conversion using fiber four-wave mixing with two orthogonal pump lights of different frequencies," J. Lightwave Technol. **12**(11), 1916–1920 (1994).
6. F. Yaman, Q. Lin, and G. P. Agrawal, "A novel design for polarization-independent single-pump fiber-optic parametric amplifiers," IEEE Photon. Technol. Lett. **18**(22), 2335–2337 (2006).
7. M. A. Foster, A. C. Turner, R. Salem, M. Lipson, and A. L. Gaeta, "Broad-band continuous-wave parametric wavelength conversion in silicon nanowaveguides," Opt. Express **15**(20), 12949–12958 (2007).
8. M. Pu, H. Hu, M. Galili, H. Ji, L. K. Oxenløwe, K. Yvind, P. Jeppsen, and J. M. Hvam, "15 THz tunable wavelength conversion of picosecond pulses in silicon waveguide," IEEE Photon. Technol. Lett. **23**(19), 1409–1411 (2011).
9. R. Salem, M. A. Foster, A. C. Turner, D. F. Geraghty, M. Lipson, and A. L. Gaeta, "Signal regeneration using low power four-wave mixing on silicon chip," Nat. Photonics **2**(1), 35–38 (2008).
10. M. A. Foster, A. C. Turner, J. E. Sharping, B. S. Schmidt, M. Lipson, and A. L. Gaeta, "Broad-band optical parametric gain on a silicon photonic chip," Nature **441**(7096), 960–963 (2006).
11. H. Rong, Y. H. Kuo, A. Liu, M. Paniccia, and O. Cohen, "High efficiency wavelength conversion of 10 Gb/s data in silicon waveguides," Opt. Express **14**(3), 1182–1188 (2006).
12. H. Hu, H. Ji, M. Galili, M. Pu, C. Peucheret, H. C. H. Mulvad, K. Yvind, J. M. Hvam, P. Jeppesen, and L. K. Oxenløwe, "Ultra-high-speed wavelength conversion in a silicon photonic chip," Opt. Express **19**(21), 19886–19894 (2011).
13. H. Ji, M. Pu, H. Hu, M. Galili, L. K. Oxenløwe, K. Yvind, J. M. Hvam, and P. Jeppsen, "Optical waveform sampling and error-free demultiplexing of 1.28 Tbit/s serial data in a nano-engineered silicon waveguide," J. Lightwave Technol. **29**(4), 426–431 (2011).
14. A. Biberman, B. G. Lee, A. C. Turner-Foster, M. A. Foster, M. Lipson, A. L. Gaeta, and K. Bergman, "Wavelength multicasting in silicon photonic nanowires," Opt. Express **18**(17), 18047–18055 (2010).

#168156 - $15.00 USD Received 8 May 2012; revised 27 Jun 2012; accepted 29 Jun 2012; published 3 Jul 2012

15. M. Pu, H. Hu, H. Ji, M. Galili, L. K. Oxenløwe, P. Jeppesen, J. M. Hvam, and K. Yvind, "One-to-six WDM multicasting of DPSK signals based on dual-pump four-wave mixing in a silicon waveguide," Opt. Express **19**(24), 24448–24453 (2011).
16. H. C. H. Mulvad, E. Palushani, H. Hu, H. Ji, M. Lillieholm, M. Galili, A. T. Clausen, M. Pu, K. Yvind, J. M. Hvam, P. Jeppesen, and L. K. Oxenløwe, "Ultra-high-speed optical serial-to-parallel data conversion by time-domain optical Fourier transformation in a silicon nanowire," Opt. Express **19**(26), B825–B835 (2011).
17. S. Gao, X. Zhang, Z. Li, and S. He, "Polarization-independent wavelength conversion using an angled-polarization pump in a silicon nanowire waveguide," IEEE J. Sel. Top. Quantum Electron. **16**(1), 250–256 (2010).
18. Q. Lin, O. J. Painter, and G. P. Agrawal, "Nonlinear optical phenomena in silicon waveguides: modeling and applications," Opt. Express **15**(25), 16604–16644 (2007).
19. Q. Liu, S. Gao, L. Cao, and S. He, "Design of low-dispersion-discrepancy silicon waveguide for broadband polarization-independent wavelength conversion," J. Opt. Soc. Am. B **29**(2), 215–219 (2012).
20. M. Pu, L. Liu, H. Ou, K. Yvind, and J. M. Hvam, "Ultra-low-loss inverted taper coupler for silicon-on-insulator ridge waveguide," Opt. Commun. **283**(19), 3678–3682 (2010).
21. P. O. Hedekvist and P. A. Anderson, "Noise characteristics of fiber-based optical phase conjugators," J. Lightwave Technol. **17**(1), 74–79 (1999).

1. Introduction

All-optical wavelength conversion (AOWC) is an important feature in future wavelength division multiplexing (WDM) networks. This functionality has been demonstrated in different devices including semiconductor optical amplifiers (SOAs) [1], periodically-poled lithium niobate (PPLN) waveguides [2], and highly nonlinear fibers (HNLFs) [3–6], based on different nonlinear effects. Recently, nonlinear effects in silicon waveguides have attracted considerable research interests due to compactness, large conversion bandwidth and complementary metal-oxide-semiconductor (CMOS) compatibility. Due to the strong light confinement in silicon waveguides with sub-micron dimensions, the group velocity dispersion (GVD), which is a critical parameter for parametric processes, can be engineered and thus one can achieve ultra-broadband wavelength conversion [7,8]. Previously, different nonlinear applications including signal regeneration [9], parametric amplification [10], wavelength conversion [11,12], ultra-fast waveform sampling, demultiplexing [13], multicasting [14,15], and serial-to-parallel data conversion [16] have been demonstrated based on four-wave mixing (FWM) processes in silicon waveguides. The FWM process is normally polarization dependent and an efficient FWM process occurs when the input signal and pump waves are both aligned to either the transverse-electric (TE) mode or the transverse-magnetic (TM) mode of the waveguide. However, a polarization-insensitive operation is desired since the state of polarization (SOP) of the input signal may fluctuate with time and distance in a real transmission system. Various polarization-insensitive FWM-based AOWC techniques have been demonstrated in HNLFs such as polarization diversity [3], co-polarized-pump [4], orthogonal-pump [5], and 45°-pump schemes [6]. An angled-pump scheme has also been proposed for polarization-insensitive AOWC in silicon waveguides [17]. However, such a technique has not yet been experimentally demonstrated in silicon waveguides.

In this paper, we report polarization-insensitive AOWC of a 10-Gb/s differential phase-shift keying (DPSK) data signal in a silicon waveguide. The silicon waveguide used in the experiment is dispersion engineered to obtain the same magnitude of GVD for TE and TM modes at a certain pump wavelength, which results in similar FWM conversion performances for these two modes. Using a single angled-pump scheme, we perform polarization-insensitive AOWC and error-free performance is achieved for the converted signals while the polarization of the input data signal is continuously scrambled. Moreover, we also demonstrate broadband polarization-insensitive AOWC with a large separation between the idler and signal utilizing a dual-pump configuration.

2. Principle of operation

FWM in a silicon waveguide (shown in Fig. 1(a)) is intrinsically a highly polarization dependent process. Usually, the pump and signal waves have to be co-polarized and both aligned to one of the fundamental waveguide modes (TE or TM modes) to get an efficient FWM, as shown in Fig. 1(b). However, if the SOP of the pump wave is intentionally set at a

#168156 - $15.00 USD Received 8 May 2012; revised 27 Jun 2012; accepted 29 Jun 2012; published 3 Jul 2012

certain angle with the TE or TM mode of the waveguide, the scheme can be made polarization insensitive [17] as shown in Fig. 1(c). The angled pump will be split into two orthogonal polarization components. If the pump polarization angle is carefully adjusted to make its power distribution between the TE and TM modes just balance the conversion efficiencies for those modes, a polarization independent conversion can be achieved. For instance, if the conversion efficiency for the TE mode is larger than that for the TM mode, then the pump polarization angle can be adjusted so that a lower power is projected along the TE mode than along the TM mode. As a result, the power of the output converted signal (idler wave), which is the sum of its TE and TM mode components, will keep constant regardless of the SOP of the input signal wave. The resultant polarization insensitive conversion efficiency and bandwidth are then mainly limited by those of the mode (TE or TM) that has the lower conversion efficiency and narrower bandwidth. Therefore, it is important to design and fabricate a silicon waveguide with similar FWM conversion performances for both the TE and TM modes in order to realize efficient polarization-insensitive AOWC.

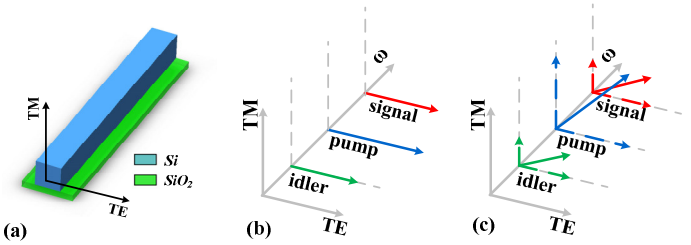

Fig. 1. (a) Schematic diagram of a silicon-on-insulator ridge waveguide. (b) Illustration of the FWM process with the signal and pump co-polarized and aligned to the TE polarization, and (c) with an angled-pump.

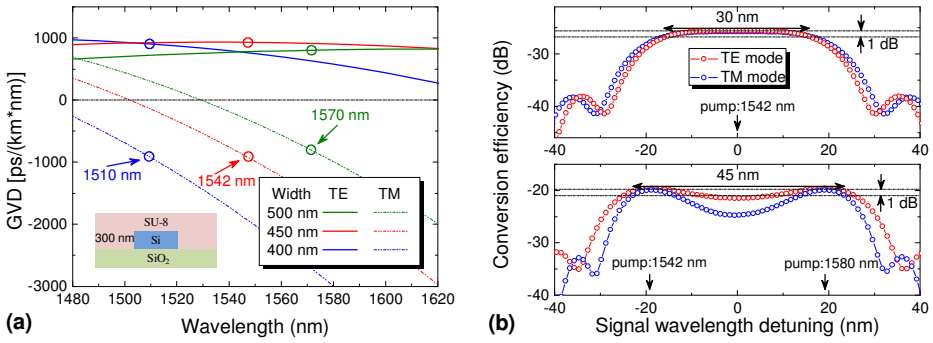

Fig. 2. (a) Simulated GVD for the TE and TM modes for silicon waveguides whose structure is represented as an inset with height 300 nm and different widths. (b) Simulated FWM conversion efficiency versus signal wavelength detuning from 1542 nm (signal pump at 1542 nm)(upper) and from 1561 nm (two pumps at 1542 nm and 1580 nm)(lower) for the TE and TM modes of the silicon waveguide of dimensions (300 × 450 nm^2).

A typical silicon waveguide has different dispersion properties for the different modes due to the structure asymmetry. However, its dispersion can be carefully engineered by tailoring the waveguide geometry to obtain similar conversion performances for the TE and TM modes when pumping at a certain wavelength. Figure 2(a) shows the calculated GVD of a silicon-on-insulator (SOI) ridge waveguide with different widths (400 nm, 450 nm, 500 nm) for both the TE and TM modes. The waveguide height is fixed at 300 nm in the calculations. As the conversion bandwidth is highly dependent on the magnitude of GVD [7], one can get similar conversion bandwidths for both the TE and TM modes if the absolute values of GVD for the different modes are comparable at the pump wavelength. As shown in Fig. 2(a), one can find a pump wavelength (denoted by circles) for the different waveguide dimensions, where the

#168156 - $15.00 USD Received 8 May 2012; revised 27 Jun 2012; accepted 29 Jun 2012; published 3 Jul 2012

GVDs for the TE and TM modes have the same magnitude but opposite sign. For example, to obtain similar conversion bandwidths for both the TE and TM modes when pumping in the C-band, a silicon waveguide, whose cross-sectional dimensions are 300 × 450 nm^2, can be used, resulting in comparable absolute GVD values for both the TE and TM modes at ~1542 nm.

Figure 2(b)(upper) shows the conversion efficiencies for the TE and TM modes as a function of signal wavelength detuning from the pump (at 1542 nm) calculated using full numerical simulations by the split-step Fourier method [12]. In the simulations, the pump power and nonlinear waveguide parameter are assumed to be 70 mW and 200 $W^{-1}\cdot m^{-1}$, respectively. As the impact of free carriers is negligible at such moderate pump powers [18], only the Kerr nonlinearity is considered in the simulations. It is observed that the conversion bandwidths for both modes are almost the same since their GVDs have the same magnitude of about 943 $ps\cdot nm^{-1}\cdot km^{-1}$ at the pump wavelength. The 1-dB bandwidth of the polarization-insensitive AOWC is expected to be ~30 nm as shown in Fig. 2(b)(upper). It is challenging to realize broadband polarization-insensitive AOWC which requires simultaneous optimization of dispersion profiles for both TE and TM polarizations for a silicon waveguide. However, one can realize polarization-insensitive AOWC with a large separation between the signal and idler by utilizing a dual-pump configuration, if the two pumps are co-polarized and their polarization angle is carefully adjusted. For example, Fig. 2(b)(lower) shows the simulated conversion efficiencies for the TE and TM modes as a function of signal wavelength detuning from 1561 nm while two pumps are used at 1542 nm and 1580 nm, respectively. Although the conversion performances for TE and TM modes are different with dual-pump configuration, which makes it more polarization sensitive and with a relatively narrow operation frequency range compared with the single-pump configuration, polarization-insensitive AOWC with a larger signal-idler frequency separation up to ~45 nm can be realized if the signal frequency is chosen close to one of the pump frequencies as shown in Fig. 2(b)(lower). The operation frequency range can be increased if the two pump frequencies are chosen in the way that the maximum absolute GVD value among different GVDs at two pump frequencies for TE and TM modes is decreased. Alternatively, the bandwidth of polarization-insensitive AOWC can be enhanced by using a waveguide with an enlarged cross-section dimension (780 × 795 nm^2), which has been theoretically demonstrated very recently in [19].

3. Experiment

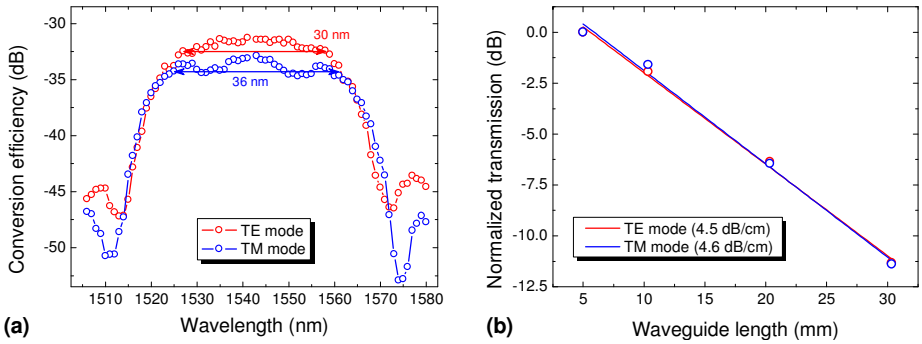

Fig. 3. (a) Measured conversion efficiency versus input signal wavelength with a fixed pump at wavelength 1542 nm for the 300 × 450 nm^2 silicon waveguide. (b) Measured transmission as a function of waveguide length for both TE and TM modes at wavelength 1550 nm.

The designed silicon waveguide is 1-cm long, inversely tapered at both ends and covered by a polymer waveguide for efficient fiber-to-chip coupling [20]. The insertion loss of the device is about ~8 dB. Figure 3(a) shows the measured conversion efficiency ($P_{out\text{-}idler}/P_{out\text{-}signal}$) as a function of signal wavelength in a CW pump-probe configuration as in [8], when the pump and signal are both aligned with either the TE or the TM mode. In the measurement, the pump wavelength and power are 1542 nm and 17.9 dBm, respectively. The 1-dB conversion

#168156 - $15.00 USD Received 8 May 2012; revised 27 Jun 2012; accepted 29 Jun 2012; published 3 Jul 2012

bandwidths for TE and TM modes are 30 nm and 36 nm, respectively. Therefore, the estimated bandwidth for polarization-insensitive AOWC is ~30 nm. The maximum conversion efficiencies for the TE and TM modes are −31.2 dB and −32.9 dB, respectively. The small efficiency difference is partly due to the different fiber-to-chip coupling efficiencies [20] and propagation losses for different waveguide modes. The propagation losses for TE and TM modes are measured to be 4.5 ± 0.1 dB/cm and 4.6 ± 0.1 dB/cm, respectively, using the cut-back method as shown in Fig. 3(b).

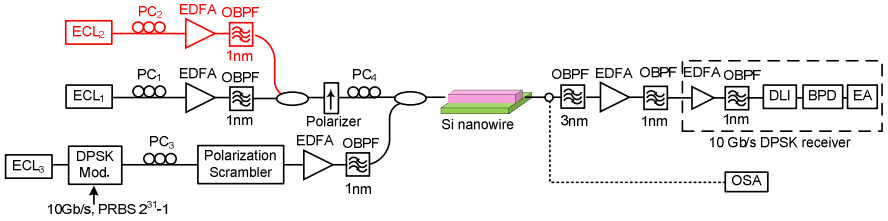

Fig. 4. Experimental setup for polarization insensitive wavelength conversion of a 10-Gb/s DPSK data signal in a silicon waveguide. The components represented in red are used optionally for the dual-pump conversion experiment.

The experimental setup for polarization-insensitive AOWC of a 10-Gb/s DPSK signal in a silicon waveguide is shown in Fig. 4. The set-up is designed so as to allow either single angled-pump polarization insensitive AOWC, or dual-pump conversion, as described later. The pump waves are generated from external cavity lasers (ECL_1 and ECL_2). The signal wave, generated by ECL_3, is externally modulated by a Mach-Zehnder modulator (MZM) with a 10-Gb/s DPSK signal, encoded with a pseudo-random binary sequence (PRBS) of length 2^{31}-1. In order to test the polarization sensitivity, the SOP of the signal is continuously scrambled over the entire Poincaré sphere with a frequency of the order of 700 kHz-1 MHz. All the pump and signal waves are amplified by erbium-doped fiber amplifiers (EDFAs), filtered by 1-nm optical band pass filters (OBPFs), and then combined by 3-dB couplers before coupling into the silicon waveguide. Two tapered fibers are used for coupling light into and out of the silicon waveguide. The polarization controller (PC) is used to adjust the polarization angle for the pump. The optimum polarization angle can be found by minimizing the power variation of the converted signal (idler wave) at the output of the silicon waveguide while the input signal polarization is continuously scrambled. At the output of the silicon waveguide, the idler wave is filtered out by two OBPFs, amplified by a pre-amplifier with 25-dB gain in between, and detected by the 10-Gb/s DPSK receiver (shown by the dashed box in Fig. 4). In the receiver, the 10-Gb/s DPSK data signal is pre-amplified, filtered with a 1-nm OBPF and then demodulated by a one-symbol delay fiber interferometer (DLI). The output of the DLI is detected by a balanced photodetector (BPD), followed by a 10-Gb/s error analyzer (EA) for BER measurements.

3.1 Experiment results with a single-pump configuration

We first performed the experiment with a single-pump configuration. ECL_1 was used as the only pump wave at 1542 nm here. Figure 5(a) shows the spectrum measured at the output of the silicon waveguide with signal polarization scrambling. The pump, signal and idler waves are denoted λ_p, λ_s, and λ_i, respectively. The input powers of the pump and signal are 17.9 dBm and 9.5 dBm, respectively. Due to the degenerate FWM process, the signal is converted from 1534 nm by 15 nm to 1549 nm as shown in Fig. 5(a). The inset of Fig. 5(a) shows the measured polarization-independent conversion efficiency of the polarization-scrambled signal as a function of signal wavelength in the angled-pump case. The conversion efficiency of the generated idler is −36.5 dB. The lower conversion efficiency than the one shown in Fig. 3(a) is due to the about 3-dB lower pump power coupled to both TM or TE modes as a result of the pump field being projected nearly equally onto the two polarization modes.

#168156 - $15.00 USD Received 8 May 2012; revised 27 Jun 2012; accepted 29 Jun 2012; published 3 Jul 2012

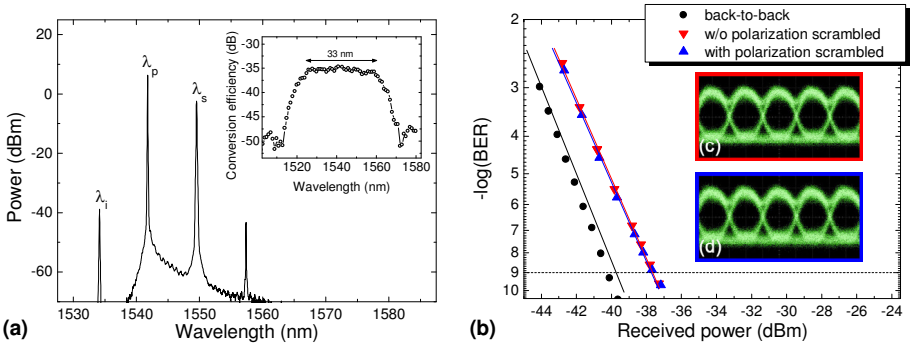

Fig. 5. (a) Measured optical spectrum at the output of the silicon waveguide for single angled-pump conversion. The inset shows the measured polarization-independent conversion bandwidth. (b) BER measurement for the 10 Gb/s DPSK back-to-back signal and the converted signal without and with the input signal being polarization-scrambled. Measured eye diagrams for the converted signal without (c) and with (d) the input signal being polarization-scrambled.

To evaluate the performance of the converted data signal and the polarization insensitivity of the AOWC, we measured the BER for the 10-Gb/s DPSK back-to-back and the converted data signals without and with signal polarization scrambling as a function of the received power measured at the optically preamplified received input. The signal polarization is in a random state when its polarization is not scrambled. As shown in Fig. 5(b), error-free operation without an error floor was achieved for the converted signal in both cases. The power penalty for the wavelength converted signal is around 2.4 dB, compared with the back-to-back case, at the BER of 10^{-9}. This is mainly attributed to the residual CW pump, whose power is ~24 dB smaller than the power of the amplified idler signal. The low optical signal-to-noise ratio (OSNR) of the converted signal also contributes to the penalty as higher OSNR helps suppressing residual pump. The receiver sensitivity for the converted signal could be improved by better filtering away the residual CW pump or increasing the pump power, which would improve the conversion efficiency and result in an increased OSNR [21]. Silicon suffers from two-photon absorption (TPA) in the telecommunication wavelength range, thus the pump power should be kept below the TPA shreshold (~39 dBm) to suppress the free-carrier induced loss [12]. However, for our current devices, the maximum launched power is limited further as a high power could result in facet damage of the polymer waveguide. This can be avoided by increasing the cross-sectional area or replacing the used polymer by a more heat-resistant material (e.g., Benzocyclobutene (BCB)). Most significantly, there is no noticeable additional power penalty caused by the polarization scrambling. Figures 5(c), 5(d) show eye diagrams of the converted 10-Gb/s DPSK data signals without and with input signal polarization scrambling, respectively. It is seen that the wavelength converted signals have clear and open eyes in both cases. As the FWM process is both amplitude- and phase-preserving, this scheme is also suitable for even more advanced modulation formats exploiting the phase dimension.

3.2 Experiment results with a dual-pump configuration

In order to achieve broadband polarization-insensitive AOWC operation, we also performed measurement using two pumps with large wavelength separation. In this measurement, the two pumps are co-polarized and also aligned to the optimum polarization angle as in the single-pump configuration. Figure 6(a) shows the spectrum measured at the output of the silicon waveguide with the signal polarization scrambled. The two CW pumps, signal and two idler waves are denoted λ_{p1}, λ_{p2}, λ_s, λ_{i1}, and λ_{i2}, respectively. The input powers of the two pumps and signal are 18.8 dBm, 16.6 dBm, and 9.5 dBm, respectively and their wavelengths are 1542 nm, 1580 nm and 1538 nm, respectively. Due to the non-degenerate FWM process, the signal is up-converted by 37 nm and 45 nm to the two idlers, respectively. This cannot be

#168156 - $15.00 USD Received 8 May 2012; revised 27 Jun 2012; accepted 29 Jun 2012; published 3 Jul 2012

achieved with a single-pump configuration since the estimated bandwidth is ~33 nm as shown in the inset of Fig. 5(a). The conversion efficiency is around −37.1 dB. We also achieved error-free operation without an error floor as shown in Fig. 6(b). All the power penalties for the wavelength-converted signal are less than 3.7 dB at the BER of 10^{-9} compared with the back-to-back case. In this case, the penalties are not only due to the residual CW pump and the limited OSNR of the converted signal, but maybe also due to the receiver sensitivity difference for signals in the C- and L-bands. Besides, the additional power penalties caused by the polarization scrambling of the signal are smaller than 1 dB. The small penalties are probably due to the polarization angles of the two pump being slightly different. We use only one polarization controller after the polarizer to adjust polarization angle for the two pumps and the polarization controller and tapered fiber to the device may be slightly wavelength dependent. As shown in Figs. 6(c)–6(f), the wavelength-converted signals have clear and open eyes, which are also comfortably error free, in all cases.

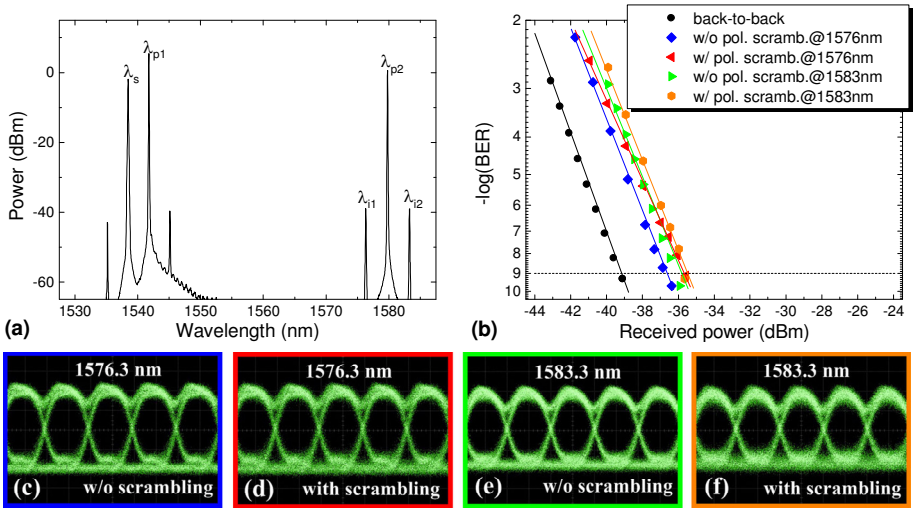

Fig. 6. (a) Measured optical spectrum at the output of the silicon waveguide for dual-pump wavelength conversion. (b) BER measurement for the 10-Gb/s DPSK back-to-back signal and the converted signal without and with the input signal being polarization-scrambled. Measured eye diagrams for the converted signal without (c, e) and with (d, f) the input signal being polarization-scrambled.

4. Conclusion

We have experimentally demonstrated polarization-insensitive AOWC of a 10-Gb/s DPSK data signal. The polarization-insensitive operation was based on angled-pump FWM in a 1-cm long dispersion-engineered silicon waveguide. Error-free performance was achieved for the wavelength converted signals regardless of whether the signal input polarization was scrambled or not in both single-pump and dual-pump configurations. The residual polarization sensitivities were very small (< 1 dB) in both cases. Polarization-insensitive AOWC with a large separation between the idler and signal was obtained with the dual-pump configuration.

#168156 - $15.00 USD Received 8 May 2012; revised 27 Jun 2012; accepted 29 Jun 2012; published 3 Jul 2012